EXPEDITED REAL TIME PROCESSING FOR THE NETL HYPER CYBER-PHYSICAL SYSTEM

Crosscutting Research

April 11th, 2019

Jesus E. Arias
Georgia Institute of Technology
Woodruff School of Mechanical Engineering
801 Ferst Dr. NW
Atlanta, GA, USA

Comas L. Haynes and Aklilu G. Giorges
Georgia Institute of Technology
Georgia Tech Research Institute
640 Strong St.
Atlanta, GA, USA

Presentation Outline

- Hybrids and Cyberphysical Systems
- Motivation
- Introduction to Hyper Facility
- Electrochemical Algorithm Optimization
- Thermal Algorithm Rediscretization
- Results
- Conclusion

SOFC/GT Hybrids

- Feature high electrical efficiency for power generation
- Compressor provides pressurized airflow to SOFC stack
- Pressurized SOFC provides thermal effluent to drive turbine
- Can use natural gas or coal syngas

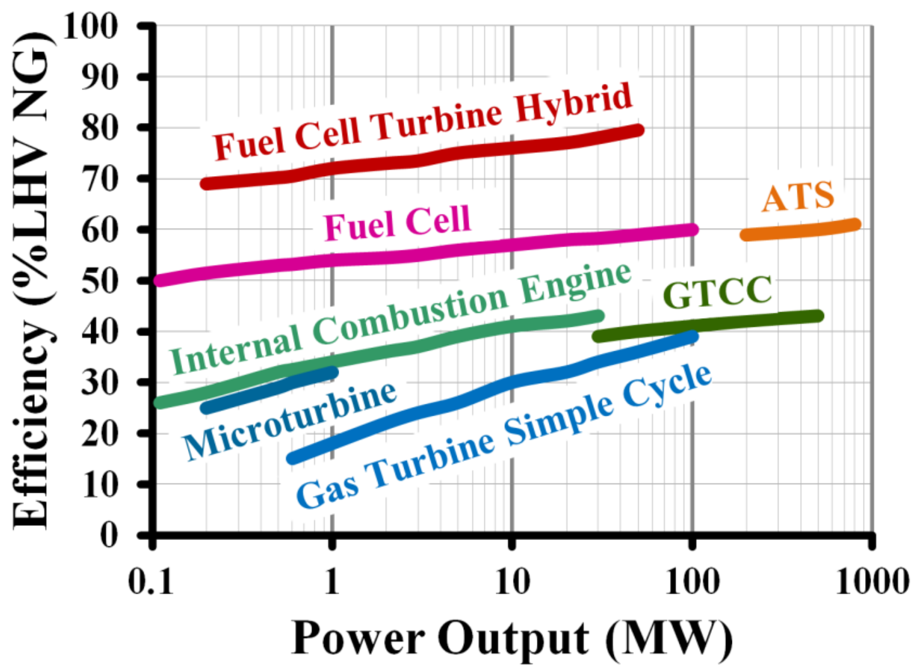

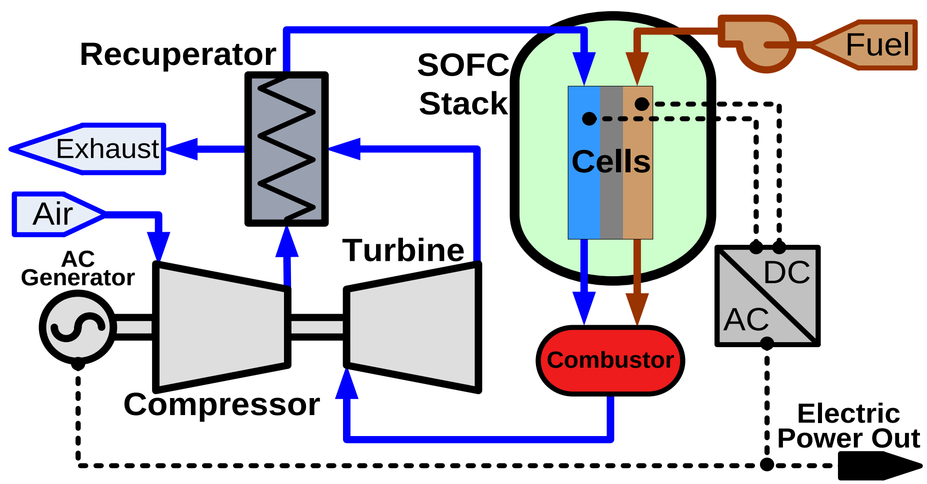

Cyber-Physical Systems

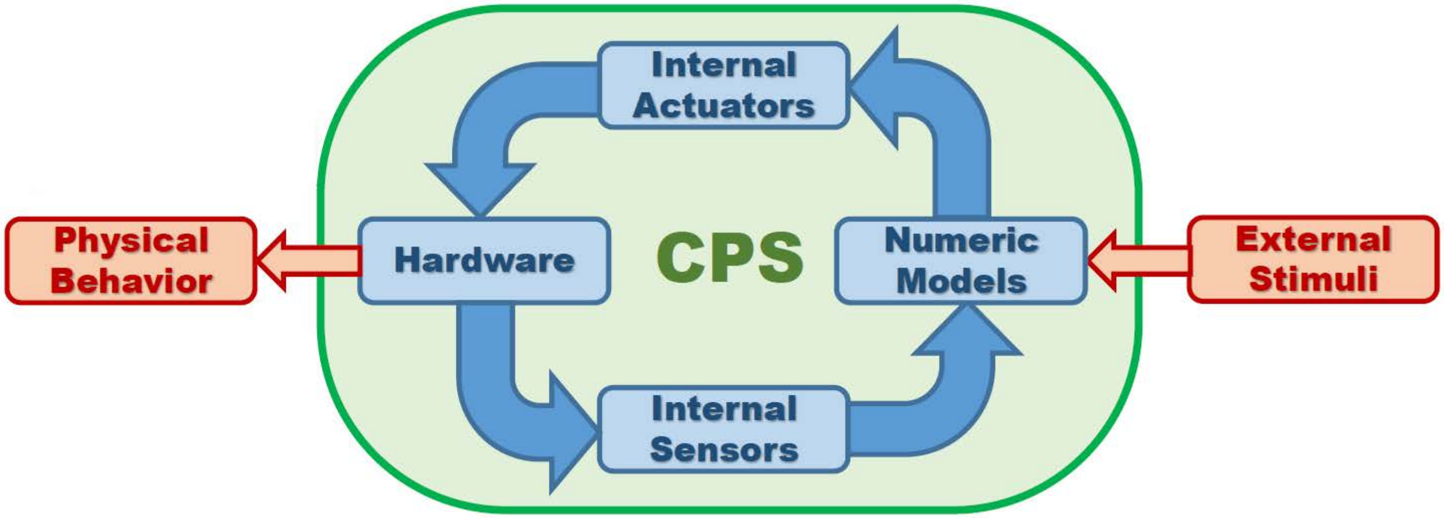

- Cyber-physical systems combine physical and virtual simulations
  - Done by coupled sensor and transfer systems
- Cost effective means to accurately test dynamic behavior
- CPS can be applied to SOFC/GT hybrids
  - SOFC thermal phenomena readily modeled by numerical simulation
  - Complex turbomachinery fluid dynamics are recreated using actual physical hardware

Motivation

- Cyberphysical systems give the ability to test systems that are cost prohibitive or not developmentally mature.
- Allows investigation of Gas Turbine/SOFC coupling in a safer and more exhaustive manner in the HyPer facility at NETL.
- Major challenge with long model computational time.
- Study focused on optimization of the SOFC model for the HyPer Facility at NETL. (Achieve below 5 ms run-time)
- Results indicate an order of magnitude reduction in calculation time.

Motivation (Technical)

"Computational predictions (e.g. **electrochemical dynamics** given load variations inclusive of mass transfer effects) and experimental measurements (e.g. **turbomachinery and flow**) inform that pivotal responses must be captured at **timescales as small as 5 msec**." *

- 5 msec is the limiting response time from turbomachinery control mechanisms. (e.g. Primary fuel valve)

- Goal is to decrease calculation time by accelerating convergence of electrochemical algorithm.

* Tucker, D., Harun, N.F., Zaccaria, V., Haynes, C., Bryden, K., " Real-Time Fuel Cell Model Development Challenges for Cyber-Physical Systems in Hybrid Power Applications," Proceedings of ASME Turbo Expo 2017: Turbomachinery Technical Conference and Exposition.

Introduction: HyPer

U.S. DEPARTMENT OF ENERGY | NATIONAL ENERGY TECHNOLOGY LABORATORY | Georgia Tech Research Institute

- Physical Gas Turbine
  - Extremely complex physics to model, reasonably affordable hardware.
- Simulated SOFC
  - Expensive hardware ($500k+), but feasible to simulate ($10k).

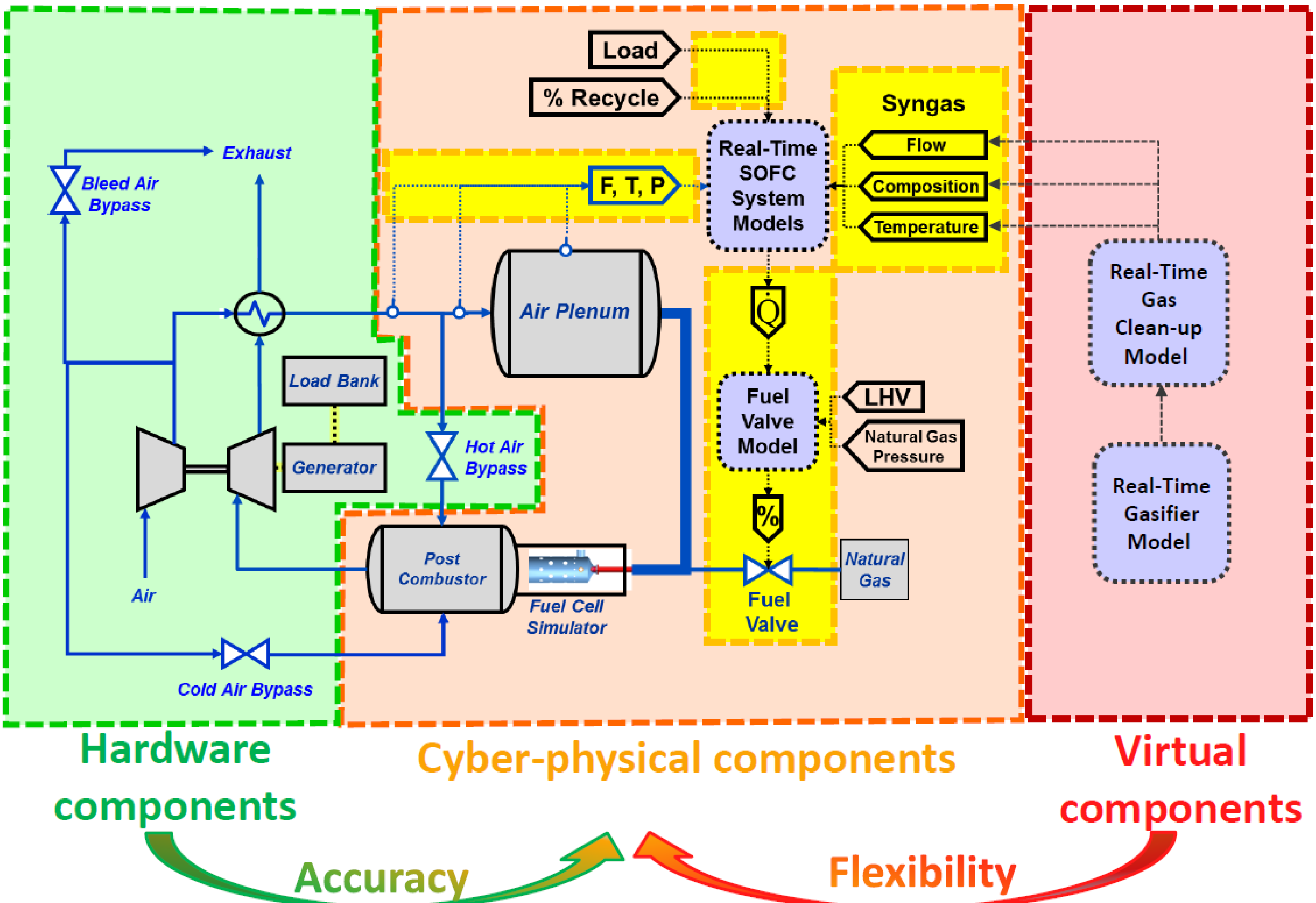

Hyper Cyber-Physical Plant

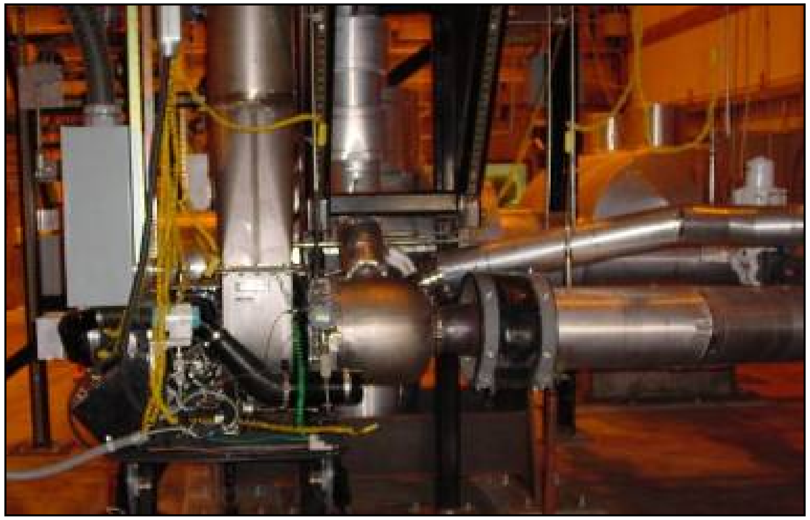

Key Approaches

- Detailed optimization of Hyper's present electrochemical algorithm
- More stable alternatives to the modified Crank-Nicolson explicit-implicit blended numerical approach that presently dictates HYPER's thermal transient profile evolutions

Method: Electrochemical

Determine Cell Voltage

- Guess overall cell voltage
- Iterate to determine correct voltage for cell load

Determine Local Current Density

- Converge upon current density for discretized cell slice
- Iterate throughout cell to determine overall cell current for set voltage

- Flowchart of iterative process for determining Voltage-Current relationship for fuel cell.
- Both use rootfinding recipes to determine values and subsequently must be solved simultaneously for a given timestep.

$$\mathrm{I(V) - I_{load} = 0} \qquad (1)$$

$$\mathrm{V(I) - V_{guess} = 0} \qquad (2)$$

- The current produced by the cell is determined by the current generated by each node at a certain voltage

$$I_{Total}(\mathrm{V}) = I_1(\mathrm{V}) + I_2(\mathrm{V}) + \cdots + I_n\ (\mathrm{V})$$

- Used to iteratively solve for cell voltage. (Eqn. 1)

- The voltage of a fuel cell V_{cell} is determined from several factors and is presented as:

$$\mathrm{V}_{cell} = \mathrm{V}(i) = \mathrm{V}_{Nernst} - \eta_{dif} - \eta_{act} - \eta_{ohm}$$

- Used to iteratively solve for local current density. (Eqn. 2)

Method: Electrochemical

Rootfinder:

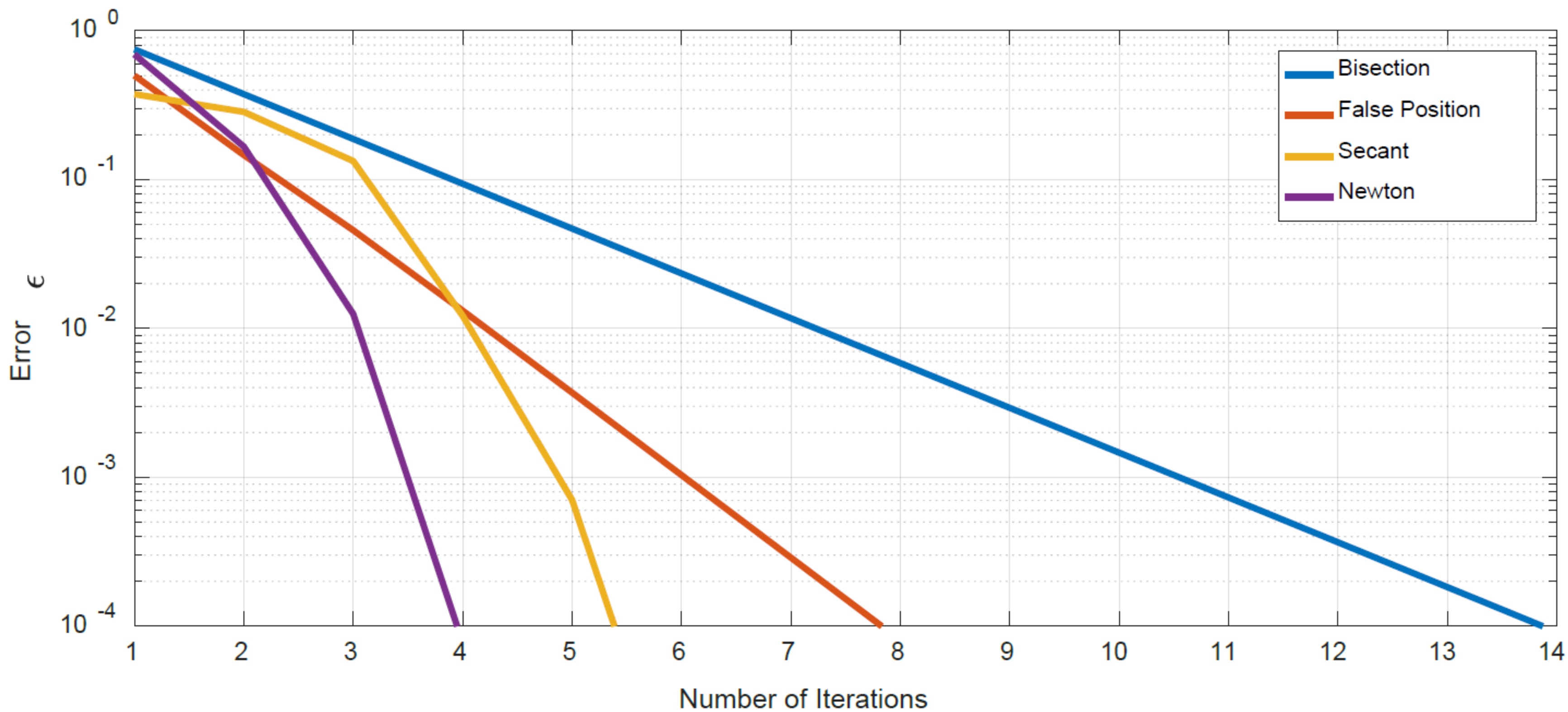

- Relative Error per Number of Iterations for different rootfinding methods.
- Illustrates the potential for optimization by using higher order rootfinding schemes.
  - Bisection requires 14 iterations vs. Secant requiring 6 iterations.
- Study performed on representative problem 0 = ln(x).

Method: Electrochemical

Cycle:

Evaluate function

$$f_c = \mathrm{I}_{\text{total}}(\mathrm{V}_c) - \mathrm{I}_{\text{target}}$$

Set up for next iteration according to (3) or (4)

Determine error ϵ

Stop if $\frac{|\mathrm{V}_c - \mathrm{V}_b|}{|\mathrm{V}_b|} \leq \epsilon$

Calculate next root

$$\mathrm{V}_c = \mathrm{V}_b - \frac{f_b \cdot (\mathrm{V}_b - \mathrm{V}_a)}{f_b - f_a}$$

False Position Method:	
If $f_a * f_c < 0$ **Then** $\mathrm{V}_b = \mathrm{V}_c$**, otherwise** $\mathrm{V}_a = \mathrm{V}_c$	(3)
Secant Method:	
$f_a = f_b, \mathrm{V}_a = \mathrm{V}_b$ $f_b = f_c, \mathrm{V}_b = \mathrm{V}_c$	(4)

- Diagram of rootfinding algorithm as implemented in voltage finding scheme.
- Implements current density estimation scheme and uses the results to allow for the implementation of higher order rootfinders. Cycle continues until a converged cell voltage is reached.

Early Termination: (Previous)

- Schematic of current density algorithm sweeping throughout the computational fuel cell nodes.

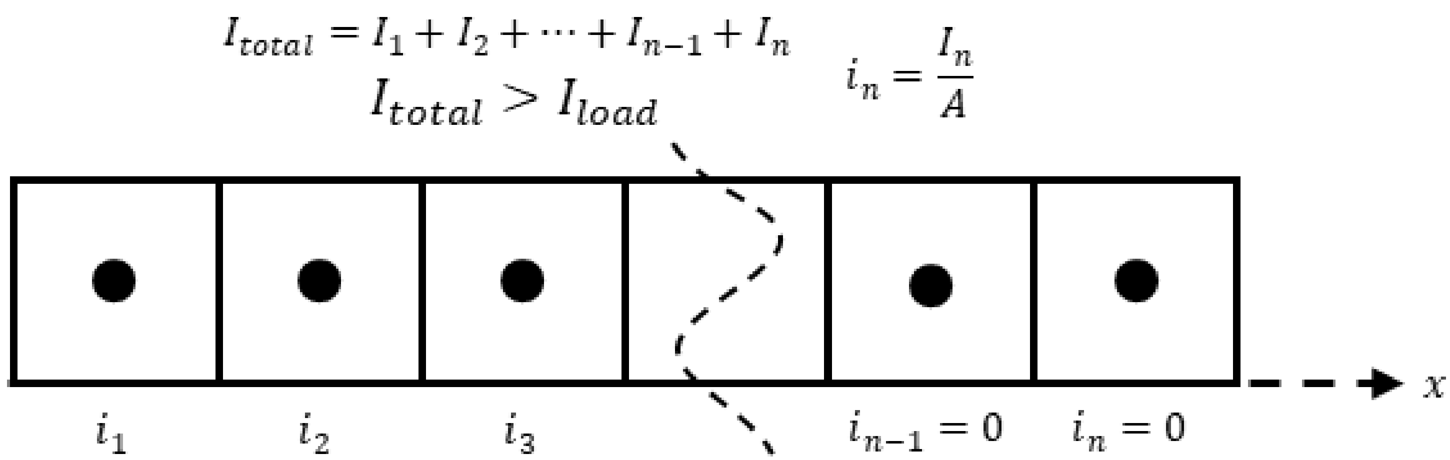

- Algorithm uses rootfinder to solve $\mathrm{V}(i_n) - \mathrm{V}_{guess} = 0$ to find local current density which is converted to the amount of current generated in the slice.
  - The slice currents are then added up to determine the total amount of current generated by the cell.
- If the calculated current becomes higher than the prescribed load the algorithm terminates early.

Method: Electrochemical

Early Termination: (New Current Estimator)

- Schematic of current density algorithm along with the current density extrapolation scheme.

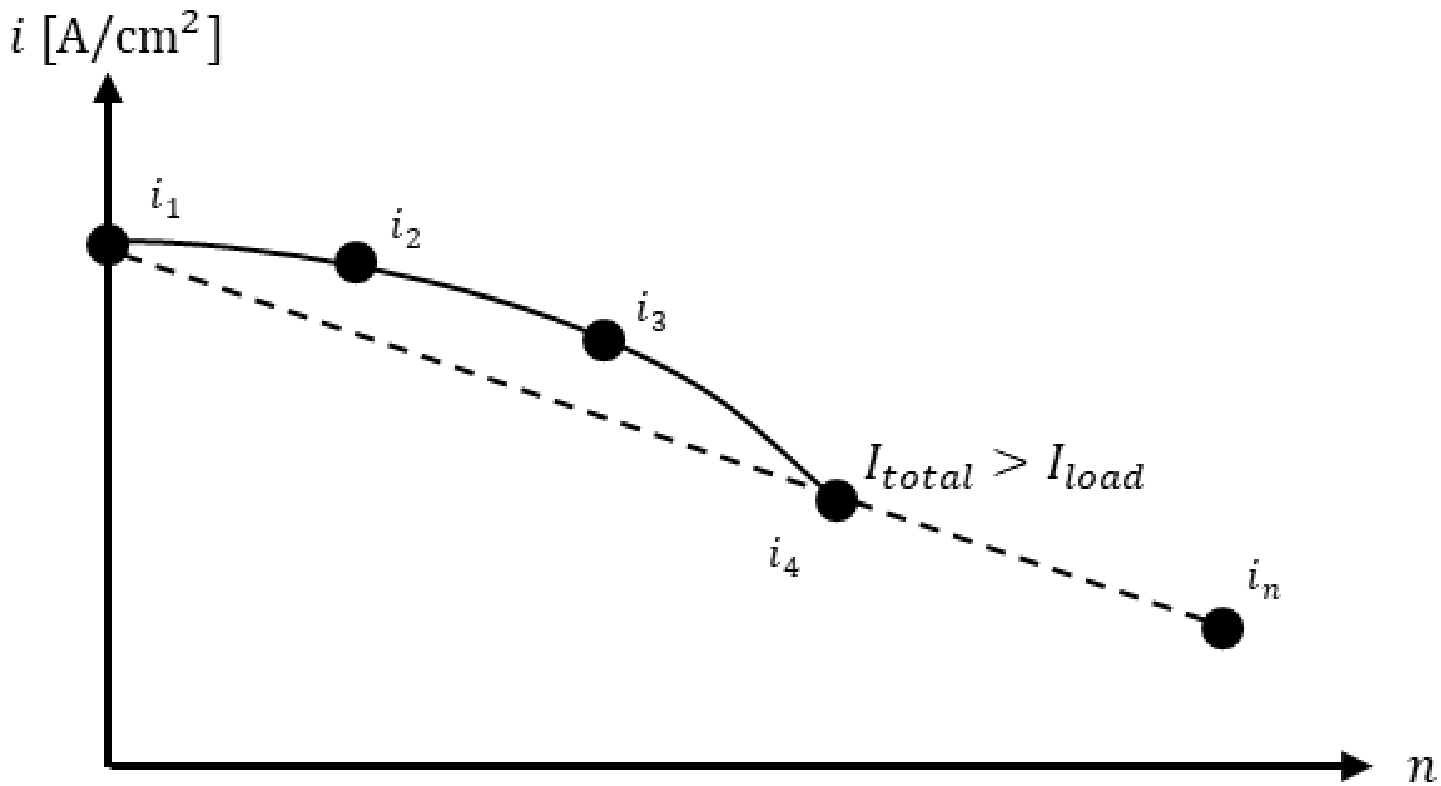

- The current density at the end of the cell is extrapolated using the current density at the first node and the current density when the total cell current surpasses the load current.
- Extrapolation disappears upon full convergence.

Replacing Thermal Algorithm

- Nodal stencil of original Crank-Nicolson (CN) scheme and new Three-Point Time Backwards Difference (TP) scheme.

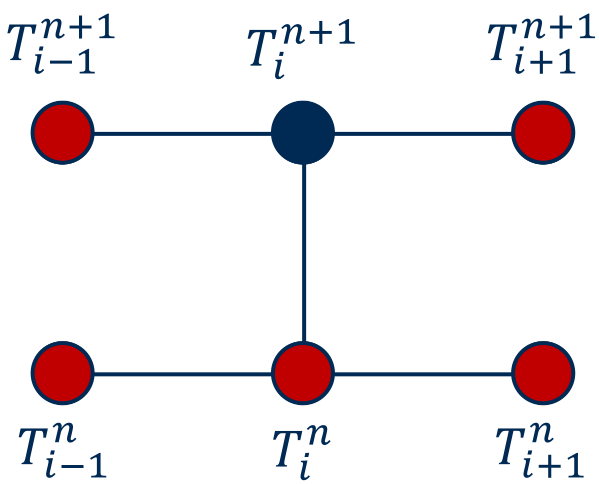

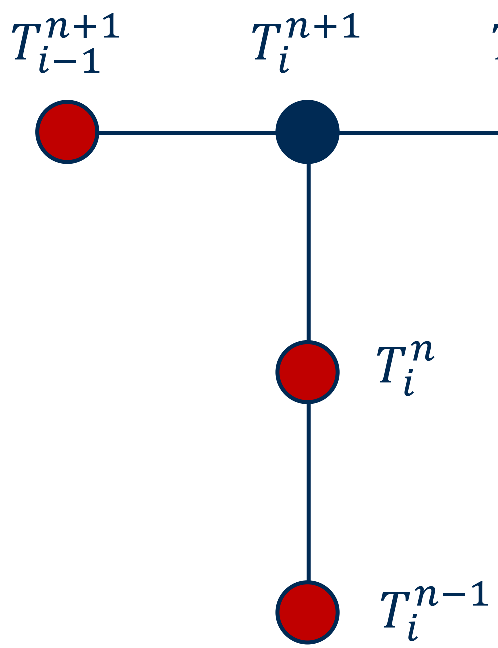

- Replaced Crank-Nicolson blended implicit-explicit scheme with fully implicit formulation
- TP is second order whereas CN in our case degenerates to first order

Results: MATLAB

Plot of average calculation time in seconds for different rootfinding methods along with the percent reduction in calculation time from baseline.

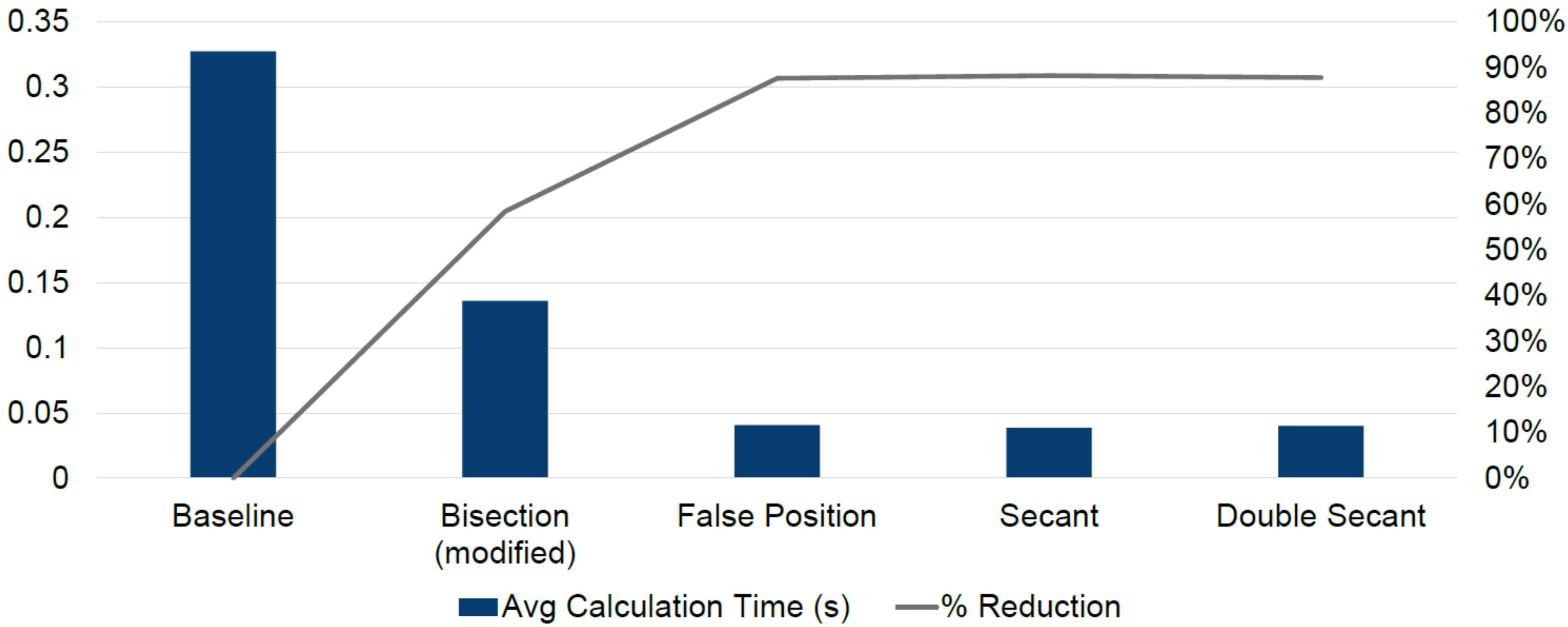

- Illustrates the drastic reduction in calculation time between baseline code and higher order methods.
- Model parameters are for a load of 250 A, 80% fuel utilization, time steps Δt of 40 ms, and input temperature of 1000 K.

Results: MATLAB

Plot of average calculation time and calculation time during a load step change event, both in seconds, and the percent relative increase in calculation time during the two events for each rootfinding scheme.

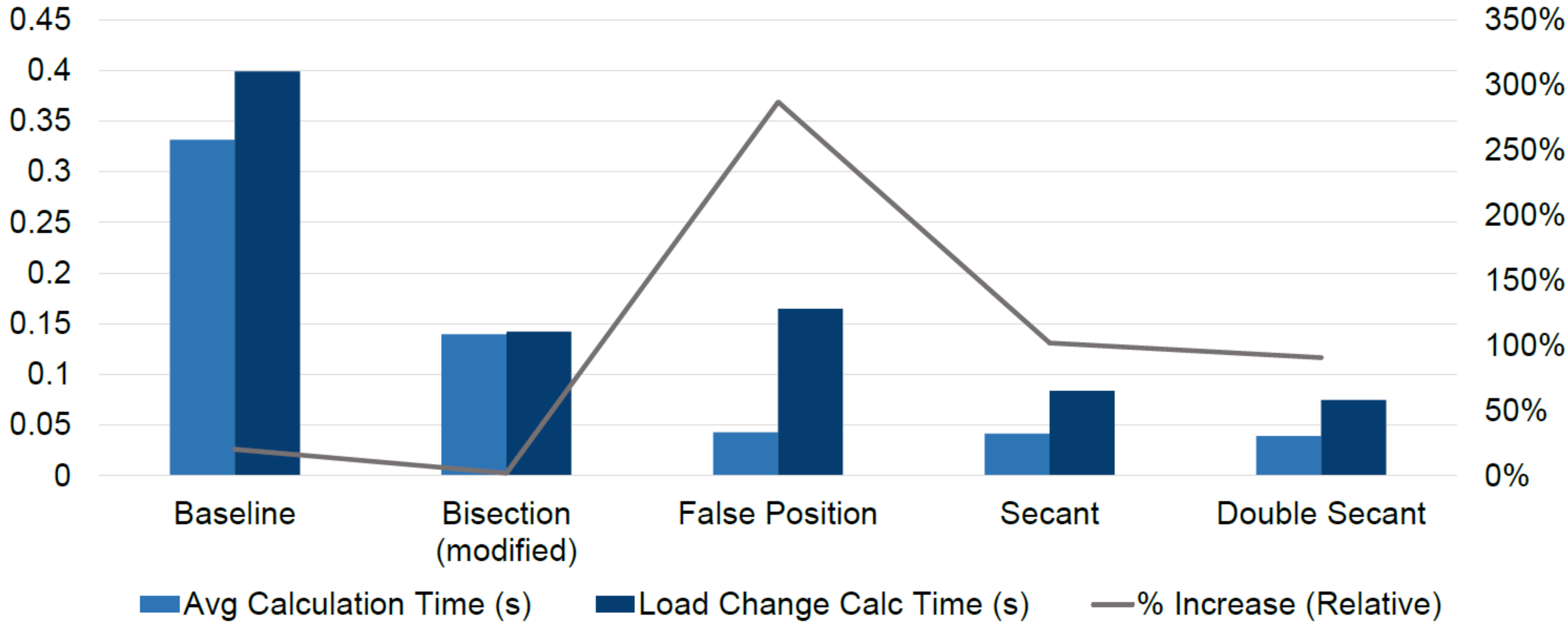

- Illustrates the drastic reduction in calculation time between baseline code and higher order methods.
- Higher order methods are more susceptible to rapid changes in inputs.
- Model parameters are for a load of 250 A at a 50% fuel utilization that is then increased to 95% fuel utilization resulting in a final load of 450 A.

Results: dSpace Offline

Plot of average calculation time in seconds for different rootfinding methods during drastic load changes. Simulation running using sample time of 80 ms.

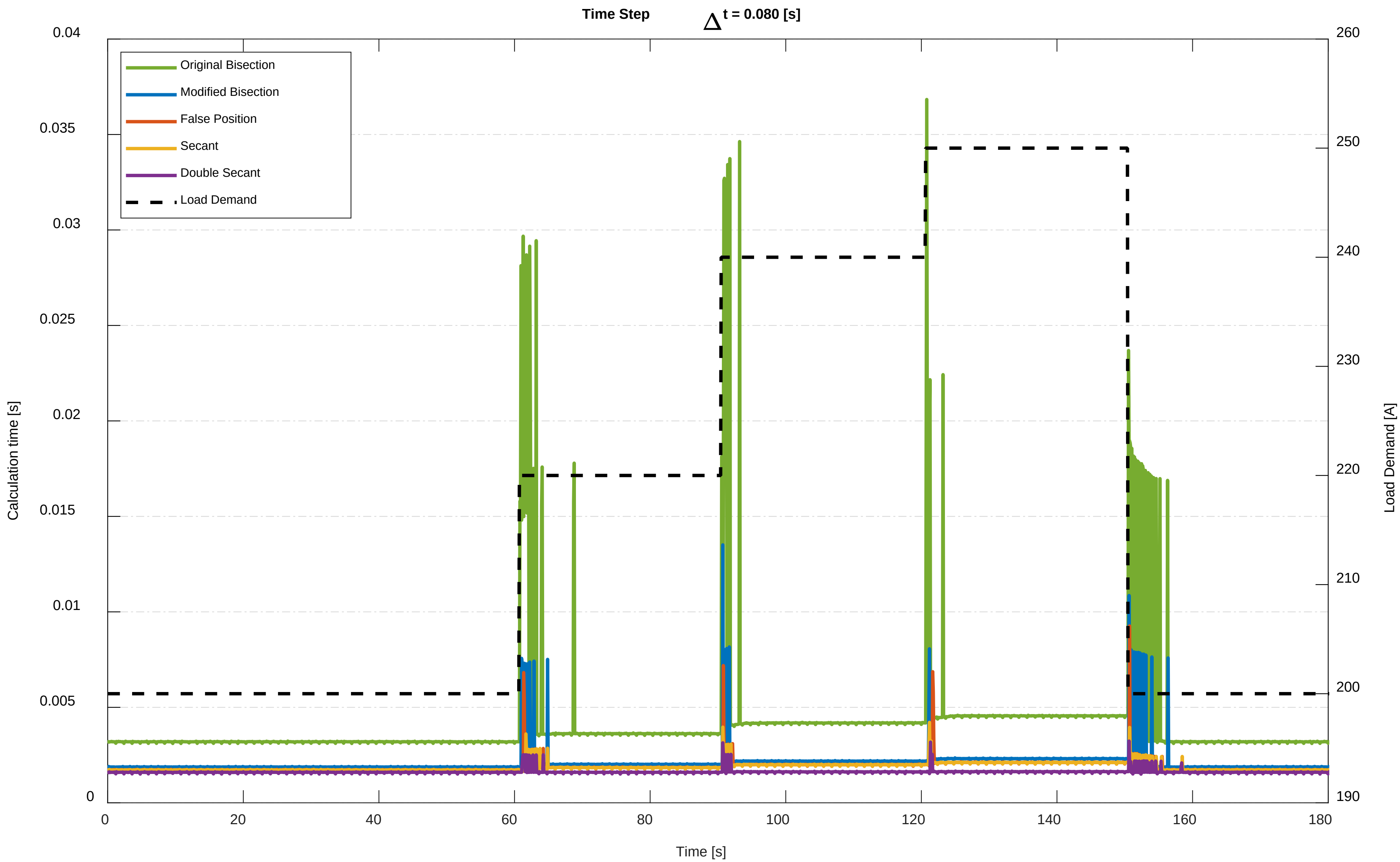

- Secant based methods are seen running below 5 ms during sharp transients. Other higher order methods also see significant calc. time reduction.

Results: dSpace Offline

Plot of average calculation time in seconds for different rootfinding methods during drastic load changes. Simulation running using sample time of 80 ms.

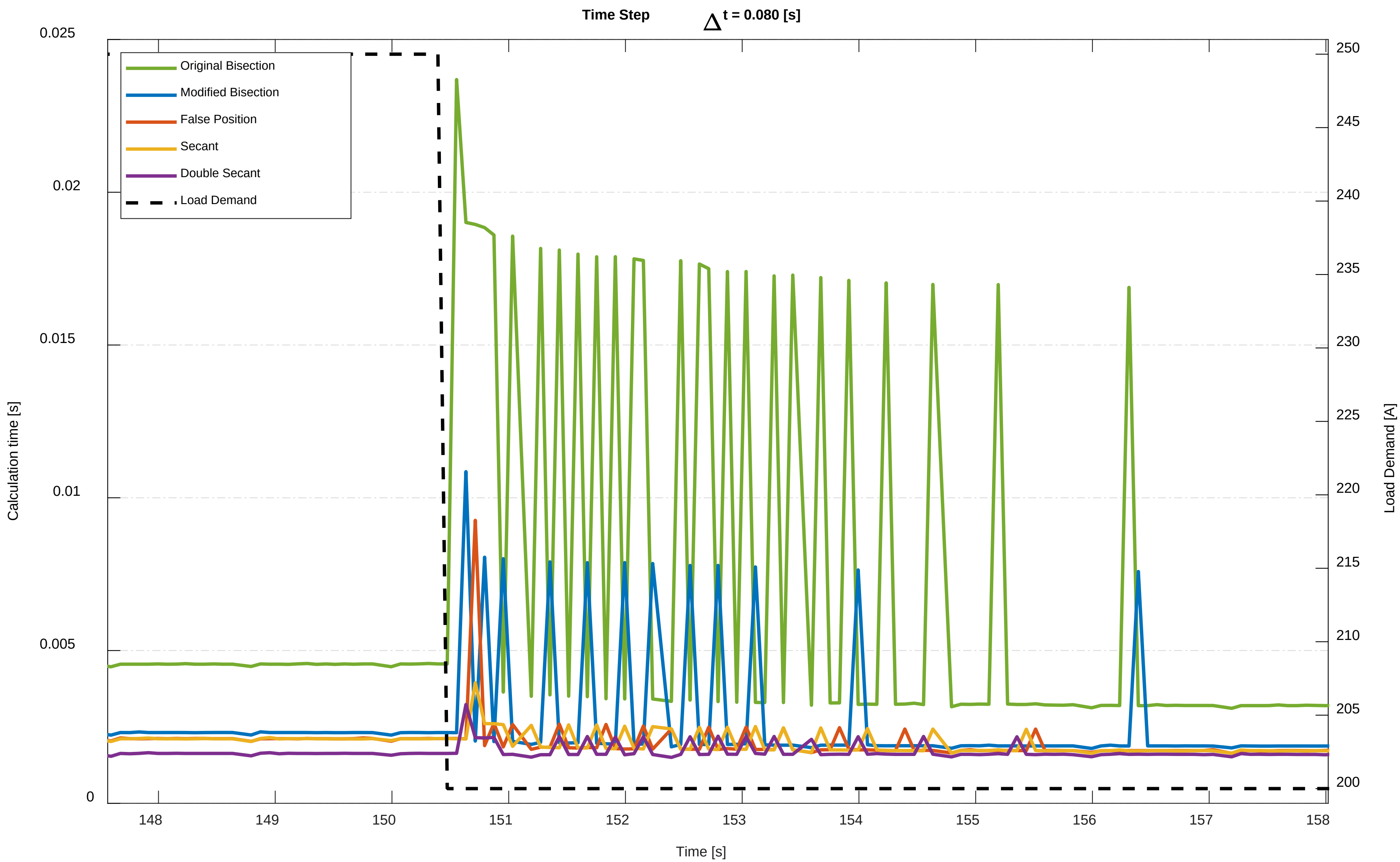

- Secant based methods are seen running below 5 ms during sharp transients. Other higher order methods also see significant calc. time reduction.

Results: dSpace Offline

Plot of average calculation time in seconds for different rootfinding methods during drastic load changes. Simulation running using sample time of 10 ms.

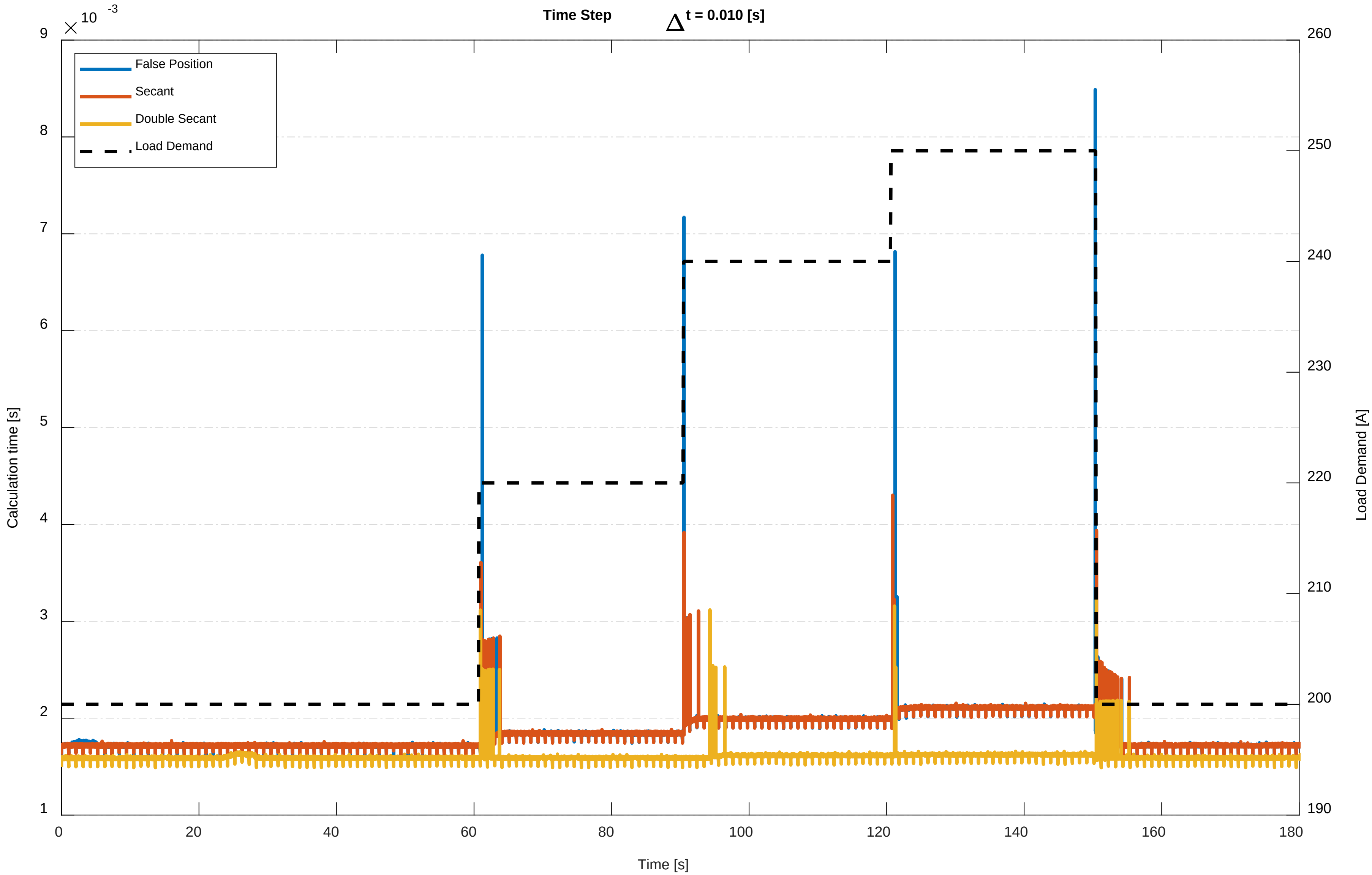

- Secant based methods are seen running below 5 ms during sharp transients. Other higher order methods also see significant calc. time reduction.

Results: dSpace Offline

Plot of average calculation time in seconds for different rootfinding methods during drastic load changes. Simulation running using sample time of 10 ms.

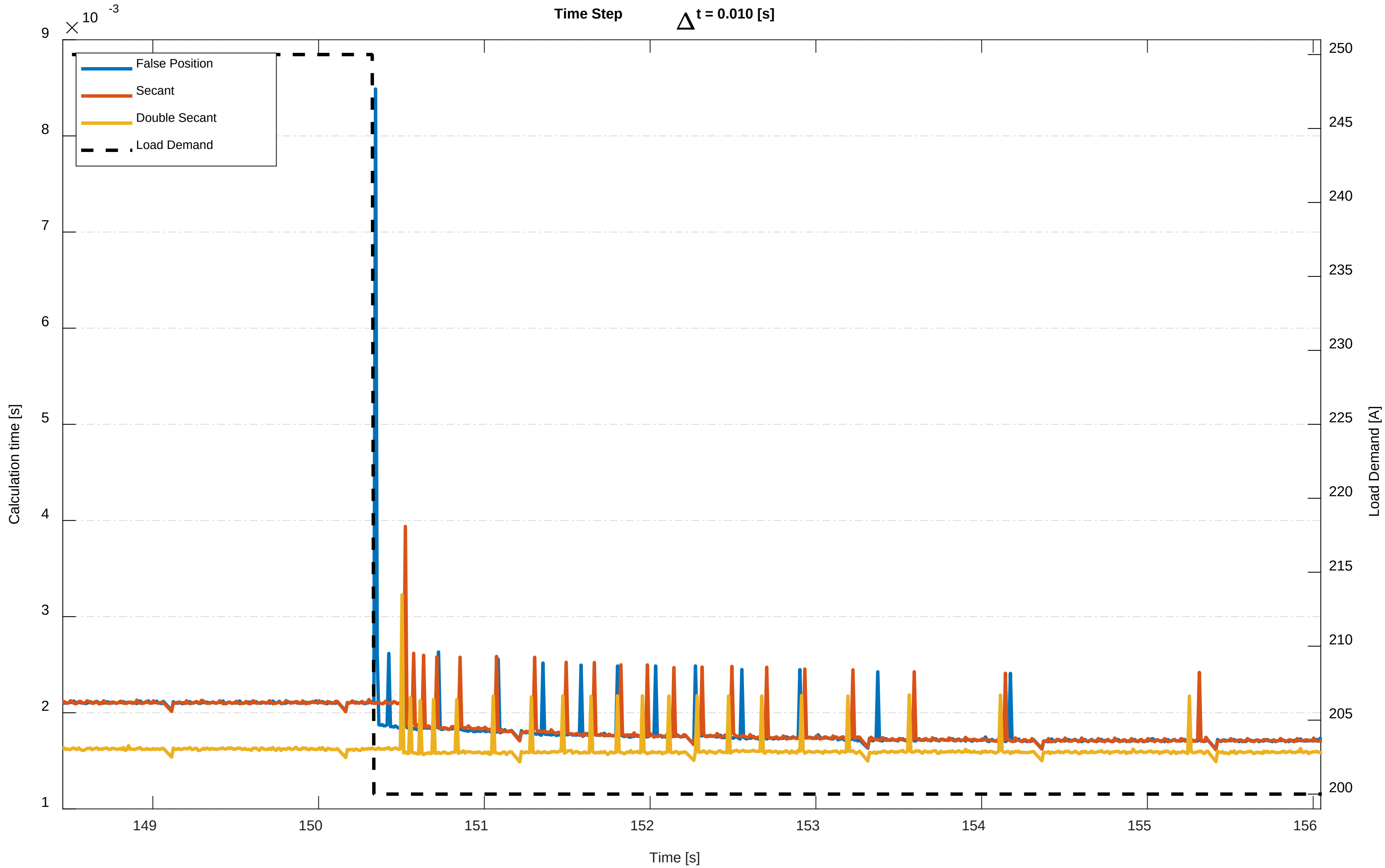

- Secant based methods are seen running below 5 ms during sharp transients. Other higher order methods also see significant calc. time reduction.

Results: dSpace Offline

Plot of maximum calculation time in seconds for different rootfinding methods during drastic load changes.

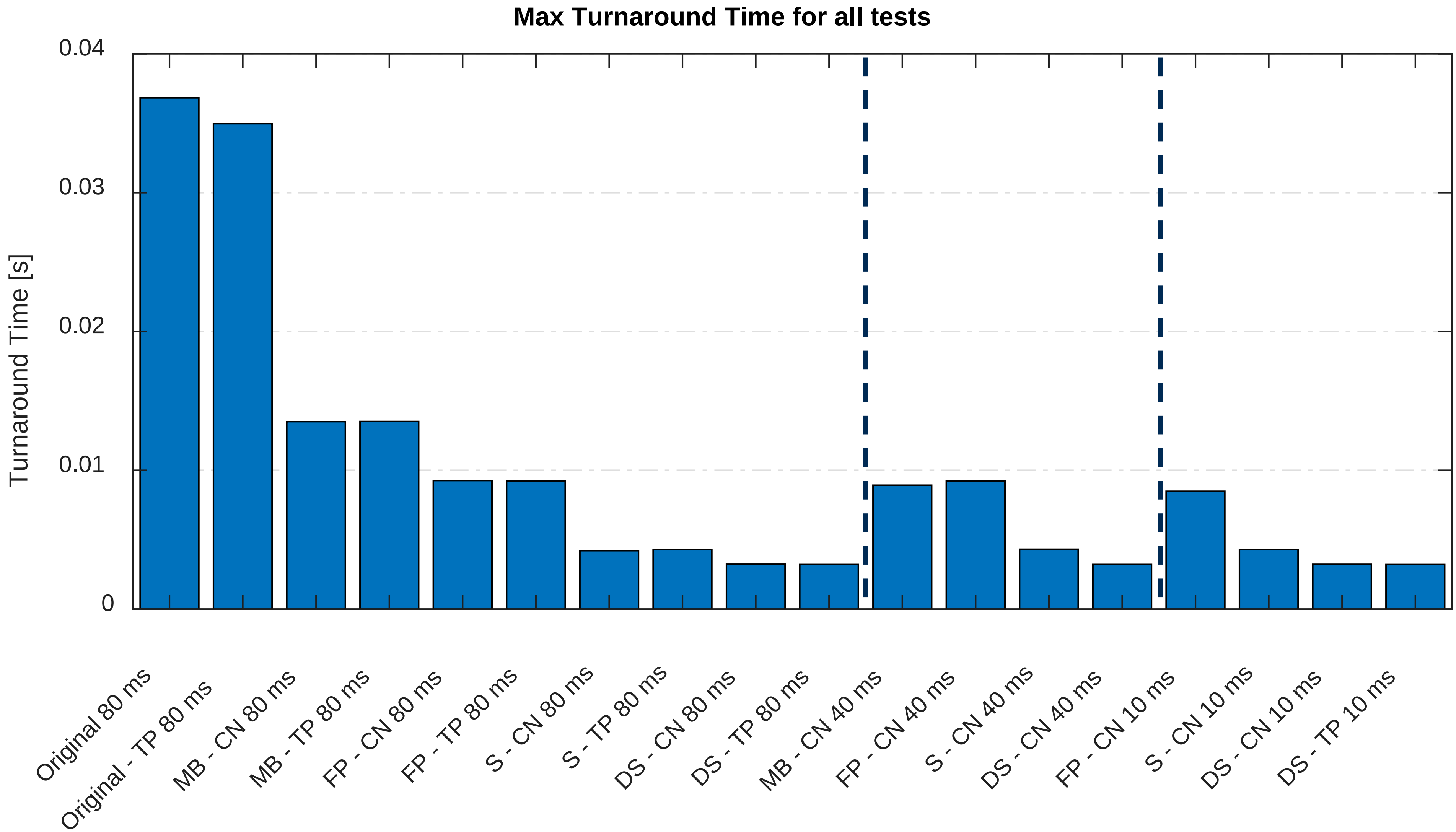

- Secant (S) and Double Secant (DS) Method is seen running below 5 ms during sharp transients both with Crank-Nicolson (CN) and Three-Point (TP). Other higher order methods also see significant calc. time reduction.

Results: dSpace Live Inputs

Plot of calculation time in seconds for different rootfinding methods during drastic load changes featuring live inputs from turbomachinery. Simulation running using sample time of 10 ms.

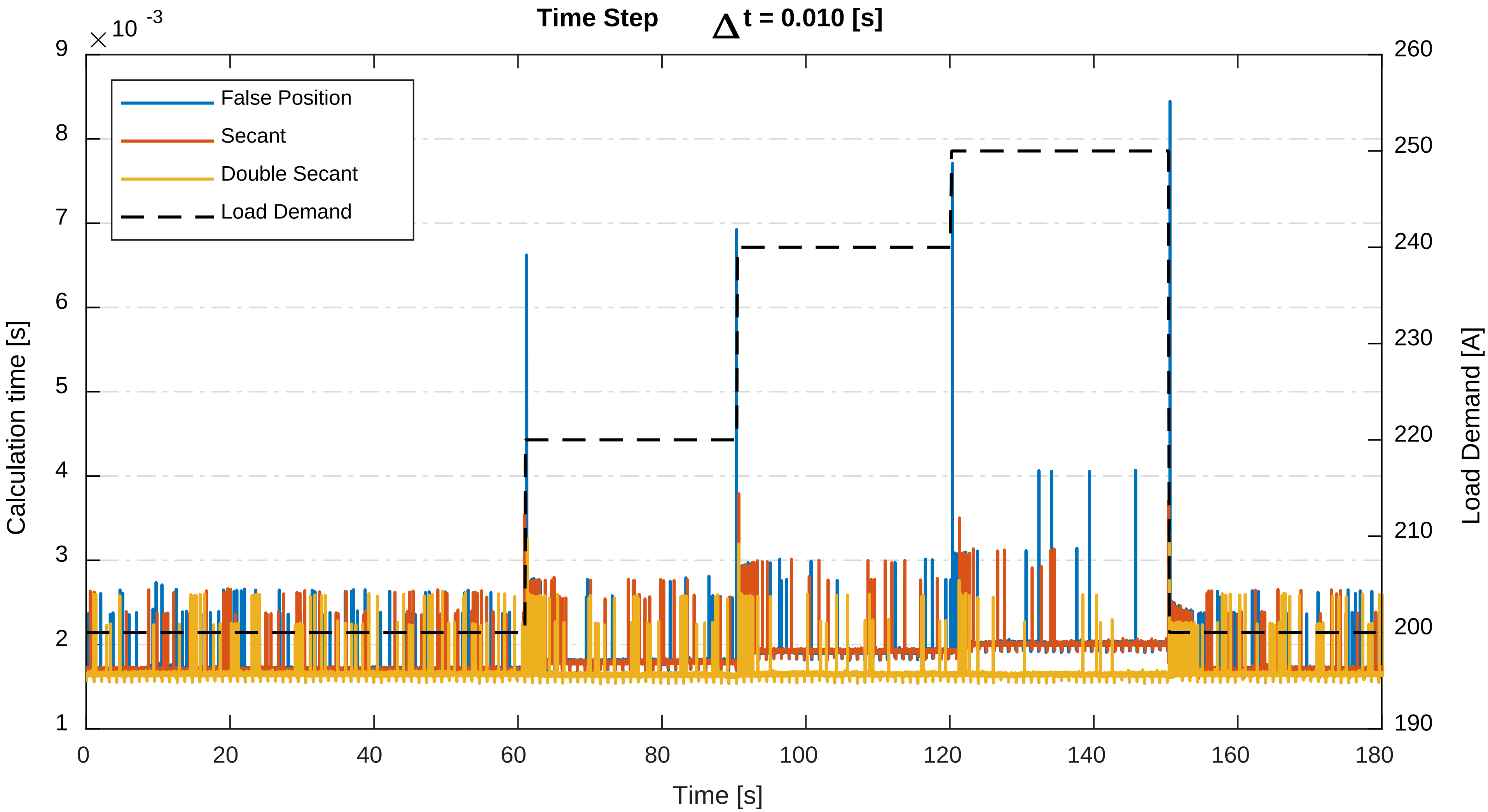

- Secant based methods are seen running below 5 ms during sharp transients. Other higher order methods also see significant reduction in calculation time.

Results: dSpace Live Inputs

Plot of calculation time in seconds for different rootfinding methods during drastic load changes featuring live inputs from turbomachinery. Simulation running using sample time of 10 ms.

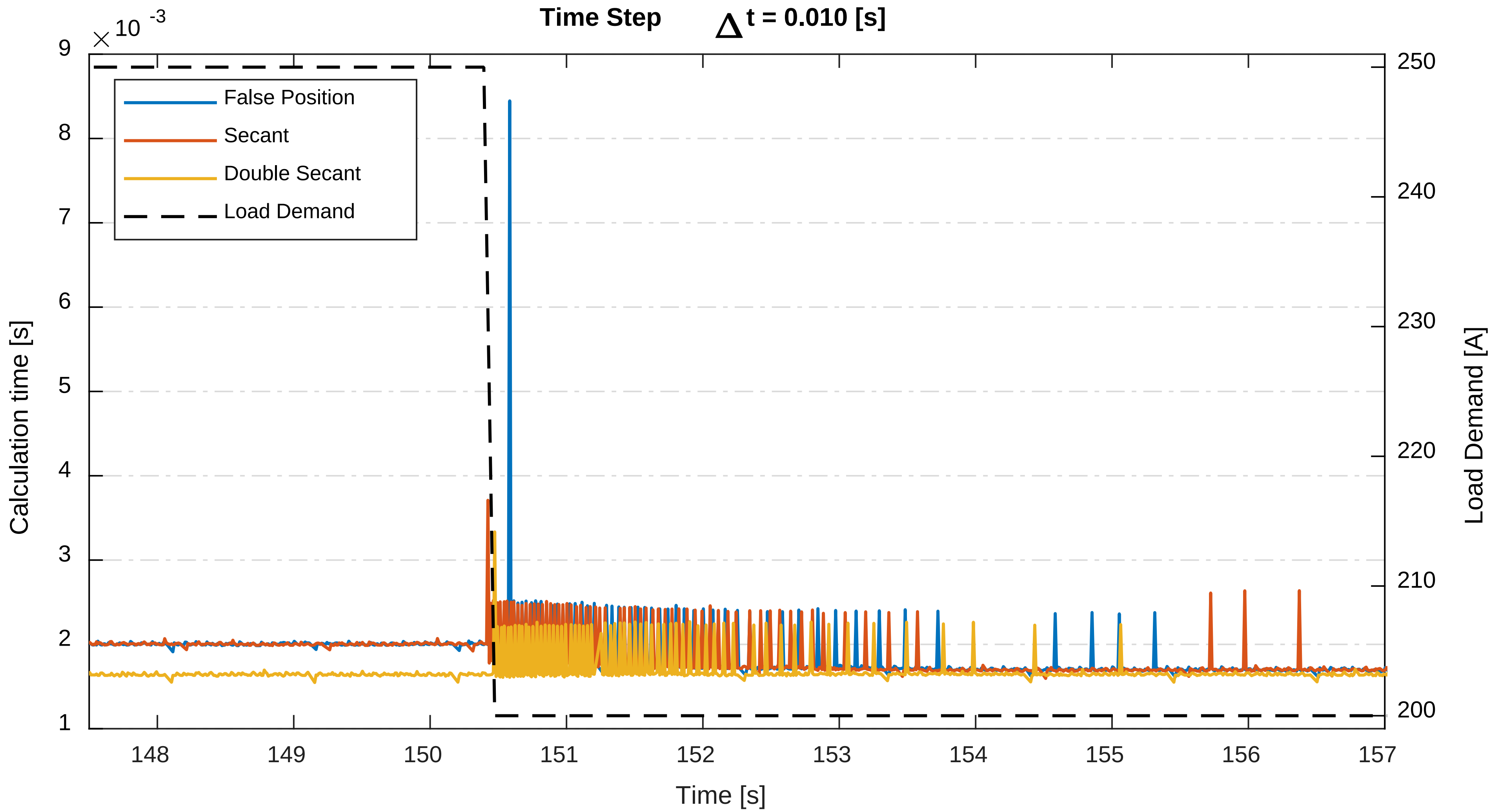

- Secant based methods are seen running below 5 ms during sharp transients. Other higher order methods also see significant reduction in calculation time.

Results: dSpace Live Inputs

Plot of maximum calculation time in seconds for different rootfinding methods during drastic load changes featuring live input data.

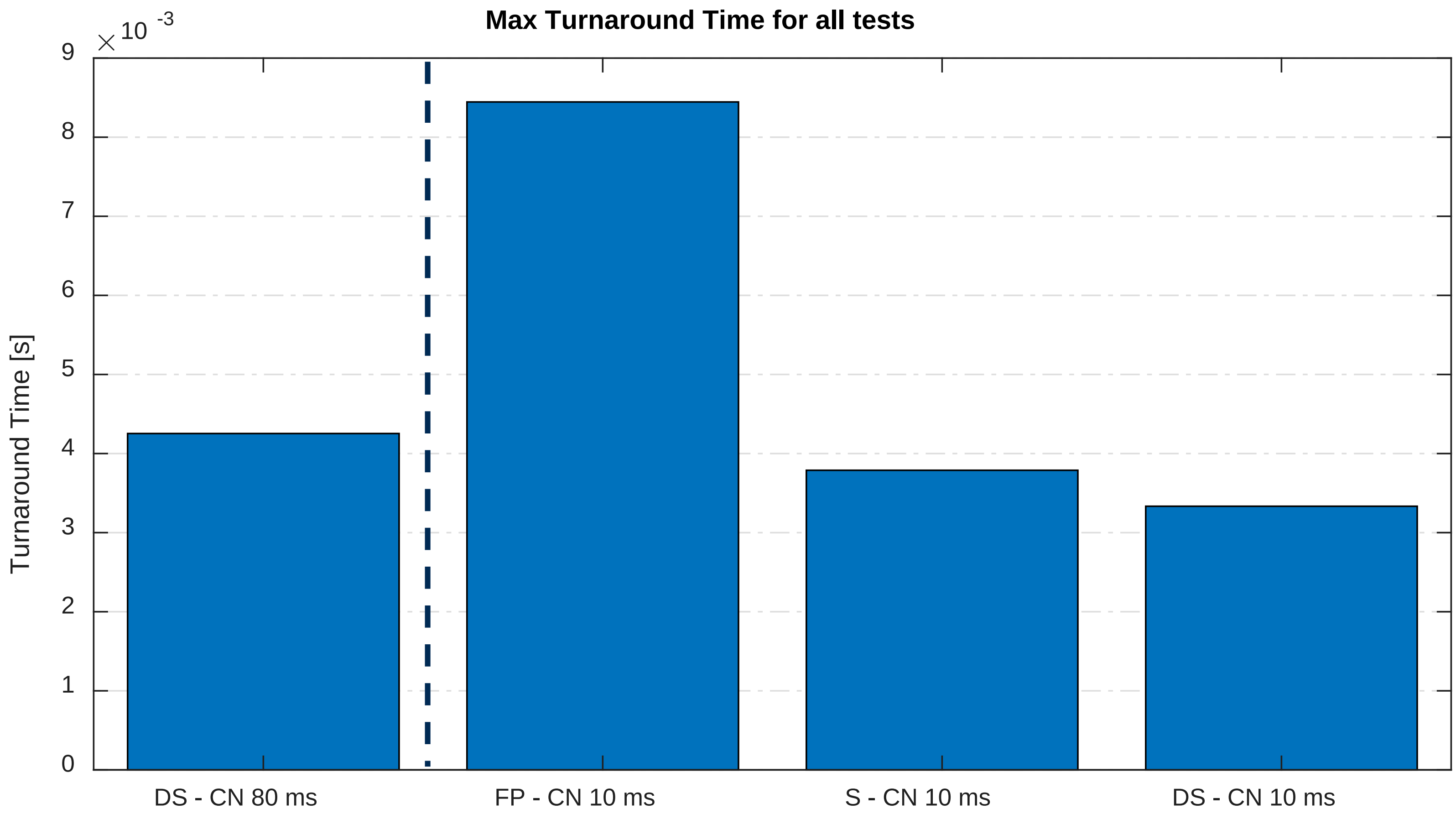

- Secant (S) and Double Secant (DS) Method is seen running below 5 ms during sharp transients. False Position (FP) fails to remain below calculation time goal

Results: dSpace Fully Coupled

Plot of maximum calculation time in seconds for different rootfinding methods during drastic load changes while fully coupled to turbomachinery.

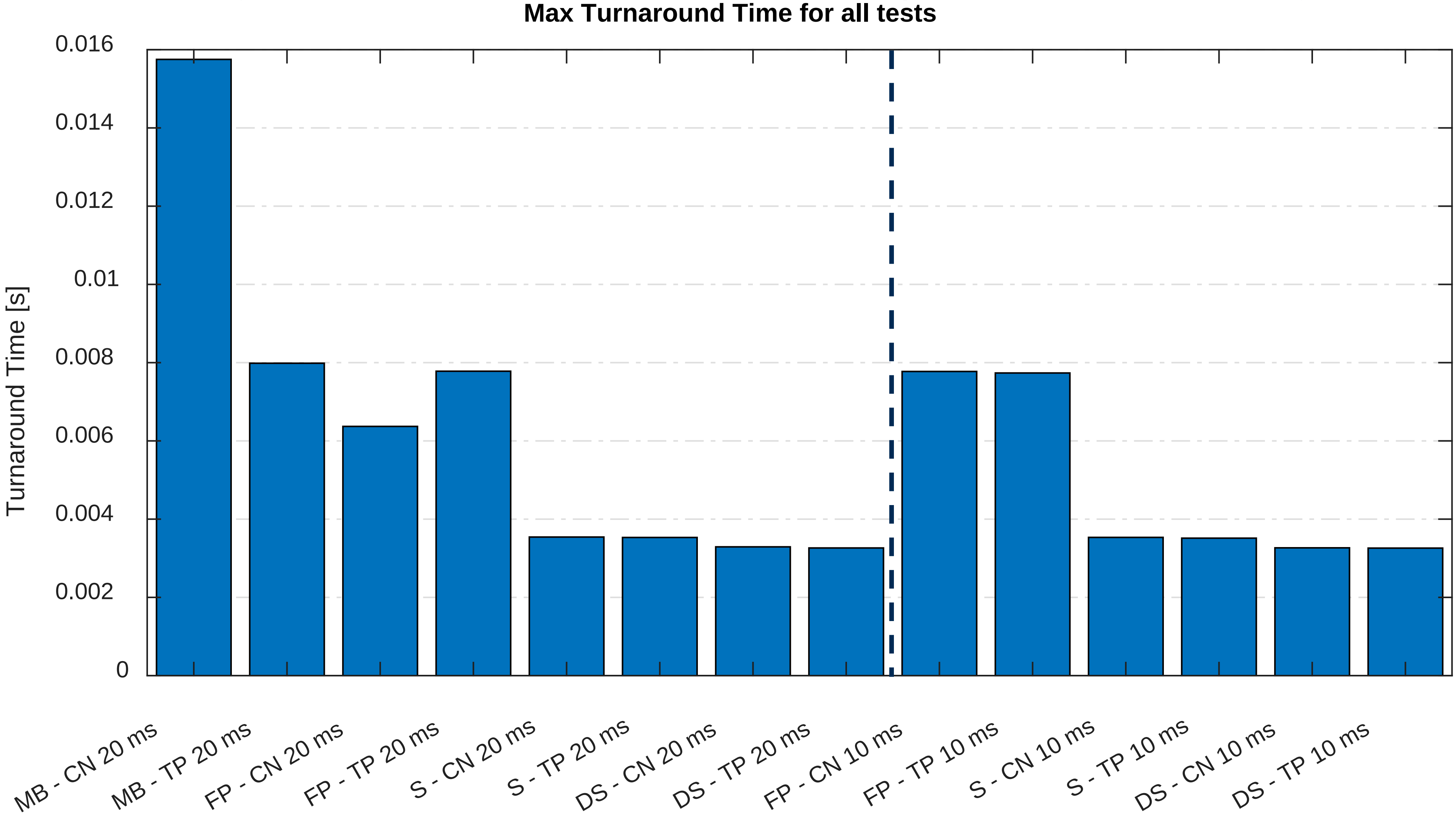

- Secant (S) and Double Secant (DS) Method is seen running below 5 ms during sharp transients both with Crank-Nicolson (CN) and Three-Point (TP). All higher order methods see significant calc. time reduction.

Results: Upgraded dSpace

Plot of maximum calculation time in seconds for different rootfinding methods during drastic load changes while fully coupled to turbomachinery.

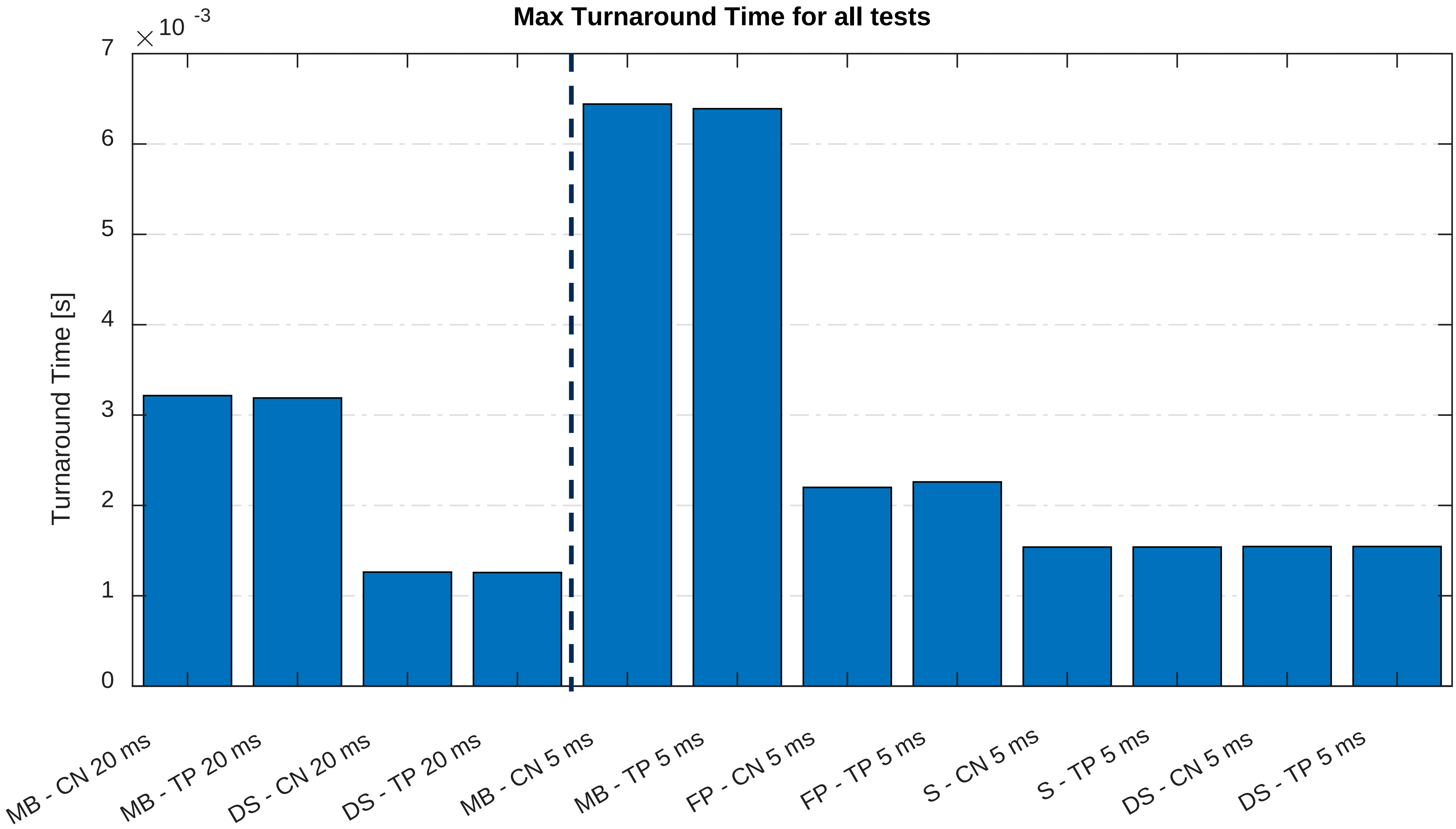

- All higher order methods show below 5 millisecond calculation times. Modified Bisection overruns under heavy transience at higher sample rates.

Conclusion

- **Calculation time** after code optimization and updated electrochemical solver is **below 5 milliseconds.**
- **New time discretization** technique when coupled with updated electrochemical algorithm is also **below 5 milliseconds.**
- With **new dSPACE hardware**, calculation time is further decreased, **nearing 1 millisecond**

Next Steps:
Introducing variable discretization, higher resolution, and more advanced gas dynamics.

Acknowledgements:

- This material is based upon work supported by the Department of Energy National Energy Technology Laboratory under Award Number DE-FE0030600.

References

[1] D. Tucker, E. Liese, J. VanOsdol, L. Lawson, and R. S. Gemmen, "Fuel Cell Gas Turbine Hybrid Simulation Facility Design," no. 36266, pp. 183-190, 2002.

[2] S. Kakaç, A. Pramuanjaroenkij, and X. Y. Zhou, "A review of numerical modeling of solid oxide fuel cells," *International Journal of Hydrogen Energy*, vol. 32, no. 7, pp. 761-786, 2007/05/01/ 2007.

[3] K. Wang *et al.*, "A Review on solid oxide fuel cell models," *International Journal of Hydrogen Energy*, vol. 36, no. 12, pp. 7212-7228, 2011/06/01/ 2011.

[4] D. Tucker, N. F. Harun, V. Zaccaria, K. M. Bryden, and C. Haynes, "Real-Time Fuel Cell Model Development Challenges for Cyber-Physical Systems in Hybrid Power Applications," no. 50831, p. V003T06A039, 2017.

[5] D. Tucker, L. Lawson, and R. Gemmen, "Characterization of Air Flow Management and Control in a Fuel Cell Turbine Hybrid Power System Using Hardware Simulation," no. 41820, pp. 959-967, 2005.

[6] D. Tucker, L. Lawson, R. Gemmen, and R. Dennis, "Evaluation of Hybrid Fuel Cell Turbine System Startup With Compressor Bleed," no. 47284, pp. 333-341, 2005.

[7] D. Tucker, L. Lawson, T. P. Smith, and C. Haynes, "Evaluation of Cathodic Air Flow Transients in a Hybrid System Using Hardware Simulation," no. 42479, pp. 585-594, 2006.

[8] D. Hughes, "A Hardware-Based Transient Characterization of Electrochemical Start-Up in an SOFC/Gas Turbine Hybrid Environment Using a 1-D Real Time SOFC Model ", George W. Woodruff School of Mechanical Engineering, Georgia Institute of Technology, Atlanta, 2011.

[9] D. Hughes, W. J. Wepfer, K. Davies, J. C. Ford, C. Haynes, and D. Tucker, "A Real-Time Spatial SOFC Model for Hardware-Based Simulation of Hybrid Systems," no. 54693, pp. 409-428, 2011.

[10] T. P. Smith, "Hardware Simulation of Fuel Cell/Gas Turbine Hybrids," George W. Woodruff School of Mechanical Engineering, Georgia Institute of Technology, Atlanta, 2007.

[11] T. P. Smith, C. L. Haynes, W. J. Wepfer, D. Tucker, and E. A. Liese, "Hardware-Based Simulation of a Fuel Cell Turbine Hybrid Response to Imposed Fuel Cell Load Transients," no. 47640, pp. 319-328, 2006.

[12] E. Süli and D. F. Mayers, *An Introduction to Numerical Analysis*. Cambridge: Cambridge University Press, 2003.

[13] R. L. Burden and J. D. Faires, *Numerical analysis*, 9th ed. Boston, MA: Brooks/Cole, Cengage Learning, 2011, pp. xiv, 872 p.